Effects of localization of the semicore density on the physical properties of transition and noble metals

2008 J. Phys.: Condens. Matter 20 235239

(http://iopscience.iop.org/0953-8984/20/23/235239)

IOP PUBLISHING JOURNAL OF PHYSICS: CONDENSED MATTER

J. Phys.: Condens. Matter **20** (2008) 235239 (5pp) doi:10.1088/0953-8984/20/23/235239

Effects of localization of the semicore density on the physical properties of transition and noble metals

Virginie Trinité, Nathalie Vast and Marc Hayoun

Laboratoire des Solides Irradiés, CEA/DSM-CNRS-Ecole Polytechnique, 91128 Palaiseau, France

Received 5 February 2008, in final form 16 April 2008
Published 13 May 2008
Online at stacks.iop.org/JPhysCM/20/235239

Abstract

We use density functional theory to study the density of the 3sp semicore states in transition and noble metals. The first objective is to understand how semicore states influence cohesive properties which mainly depend on the valence density. We define a localization radius for the semicore density which is found to be a crucial parameter and to heavily influence the cohesive properties. The localization radius is found to be controlled by the occupation numbers of the 3d states. This offers the possibility of setting criteria for the construction of accurate large core pseudopotentials freezing the semicore states, and to *a posteriori* control the use of large core pseudopotentials in the modeling. We illustrate our findings with the examples of copper and titanium.

1. Introduction

Density functional theory (DFT) is a well established framework for obtaining the ground-state properties of condensed matter from the electronic density [1, 2]. Various methods [3] have been proposed to deal with Kohn–Sham (KS) equations [2] and obtain the electronic density, among which the plane wave plus pseudopotential method has been widely used in condensed matter [4]. The reason why one can easily apply the frozen core approximation—and thus generate appropriate pseudopotentials—for the atoms of the second row in the periodic table is that the separation between core and valence states corresponds to a change in principal quantum number of the electronic shells. For most elements of the third row, however, parts of the core (3s and 3p) and valence states (3d) belong to the same shell and corresponding KS atomic orbitals show much overlap in real space (figure 1)[1]. Semicore states have been explicitly treated in calculations with all-electron approaches and local basis sets [3] or with small core pseudopotentials and plane waves or a mixed basis.

The other approach consists in keeping the semicore states frozen in a pseudopotential (frozen semicore approximation, FSCA) and treating their effects implicitly via a nonlinear core correction (NLCC) [5, 6]. The FSCA + NLCC scheme has the advantage of being computationally less cumbersome because the number of electronic states is reduced, but it has the drawback of a loss of accuracy. It has been used in magnetic materials with contradictory results: early studies found it appropriate for magnetic materials [6–8]; Moroni *et al* [9] found that magnetic properties depend much on the cut-off radius r_{NLCC} of the semicore density (SCD); and results on iron and iron compounds led to the conclusion that semicore states should rather be treated explicitly [8, 10–13], at variance with the results of [14].

In this work, the first objective is to understand how semicore states influence cohesive properties, i.e. equilibrium volumes and stabilities of the crystal phases, even if they are not chemically active. To this end, we characterize the SCD by a localization radius (LR). The LR is shown to heavily influence the cohesive properties of the solid state, and to be controlled by the occupation number of the 3d electronic states, both in the atom and in the solid. Our second goal is to set up criteria for the construction of large core pseudopotentials that reduce the loss of accuracy within the FSCA + NLCC approach. This is useful for systems with a surface or point defect where atoms far from the impurity/surface can be treated with large core pseudopotentials, while the atoms near the surface/impurity are treated with small core pseudopotentials [8]. We find that when the atomic configuration for the large core pseudopotential is chosen such that SCD localization radii are close in the atom

[1] Contrastingly, the second assumption that, the semicore Kohn–Sham energy levels are much deeper than the valence ones, is well verified, and will not be discussed here.

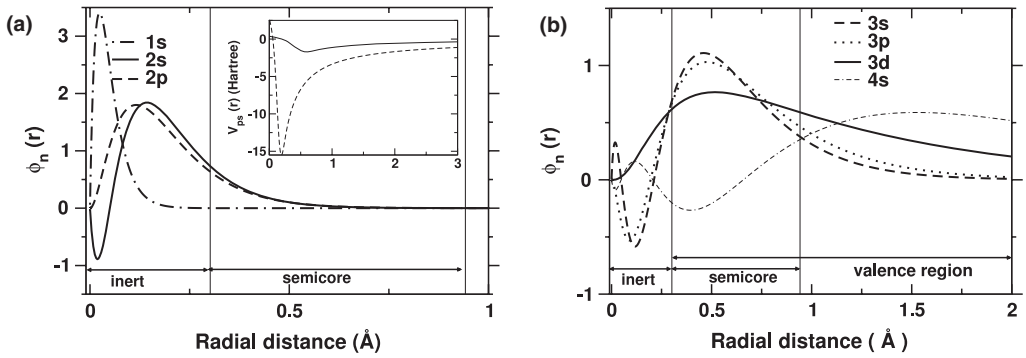

Figure 1. Atomic Kohn–Sham orbitals in titanium, as a function of the radial distance. The valence (resp. inert) region is chemically active (resp. inactive). The semicore region is chemically receptive and influences equilibrium properties (see text). (a) Core orbitals. Inset: large core ($3d^{3.5}$ $4s^{0.5}$ straight line) and small core (dashed line) pseudopotentials for the s angular momentum. (b) Semicore and valence orbitals.

Table 1. Small (SC) and large (LC) core pseudopotential parameters for the chosen atomic configurations of titanium and copper. r_{NLCC} and r^j are the cut-off radii for the SCD and for the pseudopotential of angular momentum j (in Å). $j = s$ was always taken to be the local potential. xc is the exchange–correlation functional used to unscreen the pseudopotential. LDA, local density approximation; GGA, generalized gradient approximation.

	Ti		Cu	
	SC	LC	SC	LC
Atomic config.	$3s^2 3p^6 3d^4 4s^0$	$3d^4 4s^0$ $3d^{3.5} 4s^{0.5}$ $3d^2 4s^2$ $3d^0 4s^2 4p^2$	$3s^2 3p^6 3d^{10} 4s^0$	$3d^{10} 4s^1$ $3d^8 4s^0$
r^{s}	0.26	0.79	0.21	0.79
r^{p}	0.37	0.90	0.21	0.69
r^{d}	0.26	0.26	0.13	0.13
r_{NLCC}		0.42		0.32
xc	LDA or GGA	LDA	LDA or GGA	LDA

and in the solid, or, equivalently, such that the occupation number of the 3d states are similar in the atom and in the solid, the accuracy of the pseudopotential developed in the FSCA allows one to recover the cohesive properties calculated with small core pseudopotentials.

2. Computational details

To study the effects of semicore states, we have constructed two types of pseudopotentials for titanium and copper using the Bachelet–Hamman–Schlüter method [15]. The first set consists of small core pseudopotentials in which 3s and 3p orbitals were explicitly included in the valence states. This is our reference set, whose parameters (table 1) were chosen according to the usual criteria [16]. Several sets of large core pseudopotentials have been constructed with semicore states kept frozen in the core (table 1)[2].

Our pseudopotentials are hard core [17] ones to favor high accuracy (inset of figure 1), and a large number of plane waves are needed in the basis set. The cut-off energy was 350 Ryd for titanium and 1500 Ryd for copper. For the integration [18] in the irreducible Brillouin zone, we used 95 **k** points for α titanium, and 104, 60, and 16 **k** points, respectively, for the high pressure phase ω-Ti, the high temperature structure β-Ti, and the fcc phase of copper[3]. This ensured a convergence of the total energy better than 1 meV.

Exchange and correlation (xc) were based either on the local-density approximation (LDA) [19, 20] or the generalized gradient approximation (GGA) [21]. The NLCC was used with large core pseudopotentials. We therefore took [5, 6]

$$E_{xc}(\rho_v + \rho_{sc}) \tag{1}$$

instead of $E_{xc}(\rho_v)$, where ρ_{sc} is taken to be either the SCD of the atom or the model of section 4. The SCD cut-off radius r_{NLCC} is chosen small enough to avoid any influence on the physical properties we will be discussing in this paper.

3. Semicore localization radius and 3d occupation number

We first examine the 3s and 3p KS states obtained in a calculation with our set of small core pseudopotentials. The semicore states in copper and in titanium are not chemically active[4]. But in the atom, we found the semicore states to be chemically receptive: the occupation numbers of the 3d states are found to strongly influence the semicore electronic charge density (figure 2). In order to quantify this effect, we define the localization radius as

$$\langle r \rangle = \frac{\int |\mathbf{r}| \rho_{sc}(|\mathbf{r}|)\, \mathrm{d}^3\mathbf{r}}{\int \rho_{sc}(|\mathbf{r}|)\, \mathrm{d}^3\mathbf{r}}. \tag{2}$$

[2] Transferability tests are found to be of little relevance for large core pseudopotentials, as cut-off radii cannot be chosen in the inert region of figure 1. Instead, they are close to the position of the outer node of the 4s or 4p wavefunctions (inset of figure 1).

[3] This corresponds to a $12 \times 12 \times 8$ regular mesh in the first Brillouin zone for α titanium, $8 \times 8 \times 10$ and $14 \times 14 \times 14$ for the high pressure and high temperature phases of Ti and $6 \times 6 \times 6$ for copper, respectively.

[4] (i) Semicore states do not participate in the metallic bond in the solid state. The SCD vanishes between two nearest atoms. (ii) The 3s and 3p Kohn–Sham energy levels show little dispersion in the Brillouin zone. (iii) Contrary to the valence density, the SCD is quasi-perfectly spherical around each titanium atom. The sphericity is very dependent on the distance to the nearest neighbor. This is true for all the phases of pure titanium we have inspected, where the DFT-LDA Ti–Ti bond length is larger than 2.6 Å. The charge density is found to be aspherical in titanium dioxide, where the Ti–O bond is calculated to be much shorter: 1.9 Å.

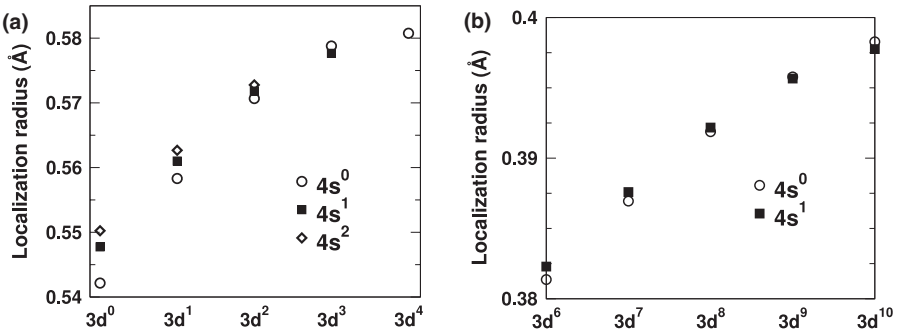

Figure 2. Localization radius (Å) as a function of the occupation number of the 3d subshell, the 4s subshell being kept empty ($4s^0$, empty circles), single ($4s^1$, filled squares) or twofold occupied ($4s^2$, empty diamonds). The 4p subshell is kept empty. (a) Ti atom. (b) Cu atom.

Table 2. Titanium: localization radius of the semicore density $\langle r \rangle$ (Å), bulk modulus B_α (GPa) of the α phase, equilibrium volumes $V_{\rm eq}$ (Å^3/atom) and total energy differences (meV/atom) of the α, ω and β phases for small core pseudopotentials in the GGA or LDA, and for large core pseudopotentials constructed from two atomic configuration: the optimal one, $3d^{3.5}4s^{0.5}$, or the $3d^04s^24p^2$. Experimental data are given when available.

			FSCA + NLCC		
	GGA	LDA	$3d^{3.5}4s^{0.5}$	$3d^04s^24p^2$	Exp.
$\langle r \rangle$	0.57	0.58	0.58	0.55	
$V_{\rm eq}^\alpha$	17.29	16.01	16.33	18.64	17.55[a]
$V_{\rm eq}^\omega$	17.02	15.78	16.12	18.49	17.26[b]
$V_{\rm eq}^\beta$	17.20	15.75	16.08	18.65	17.39[c]
B_α	115	129	129	135	110[d]
$E_\omega - E_\alpha$	−5	−23	−25	47	13[e]
$E_\beta - E_\alpha$	108	91	89	83	71[f]

[a] Reference [22].
[b] $T = 0$ K extrapolation of [23].
[c] $T = 0$ K extrapolation of [24]. (The linear expansion coefficient of the ω phase is unknown and has been approximated by the linear expansion coefficient of the α phase of [23].)
[d] $T = 4$ K in [25].
[e] The value is deduced from the data of [31], [30], see reference [48].
[f] $T = 0$ K extrapolation of [26].

The LR decreases by as much as 7% between $3d^0$ and $3d^4$ in titanium (figure 2(a)). In copper, the decrease in the LR between the filled d band and the $3d^6$ configuration is also noticeable (figure 2(b)), although two times smaller: the smaller the occupation number of the d subshell, the greater the variation of the LR. At variance with these findings, the 4s occupation number (and the 4p one, not shown) only weakly affects the LR (figure 2). By tuning the 3d subshell occupation number we are able to control the LR.

We then turn to the solid state, and evaluate the occupation number in our reference calculation—with the small core pseudopotentials—by projecting the KS eigenfunctions on a set of orthogonalized atomic orbitals [27]. For the α, ω and β phases of titanium, we find the valence occupation numbers to be $3s^23p^63d^{3.5}4s^{0.5}$ both in the LDA and the GGA, comparable to the experimental [28] data $3d^34s^1$. The relaxed SCD has a LR $\langle r \rangle = 0.58$ Å, similar in the LDA and GGA (table 2 and figure 3, filled circle), and in the atomic calculation with configuration $3d^{3.5}4s^{0.5}$ (table 2). We thus conclude that the relation between the 3d occupation number and the SCD localization radius also holds in the solid.

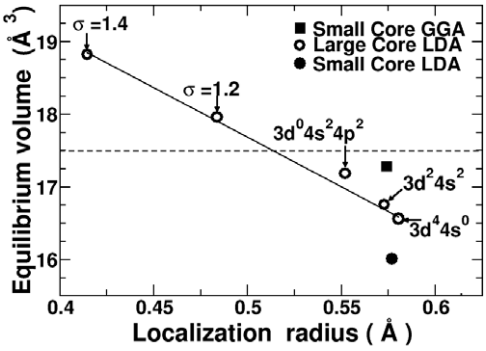

Figure 3. α-Ti: equilibrium volume as a function of the localization radius of the semicore density. Filled circle and square: LDA and GGA results with the small core pseudopotentials, respectively. Empty circles: NLCC large core pseudopotentials, with the SCD taken from an atomic calculation or from the model of equation (3). The $3d^4\ 4s^0$ configuration corresponds to $\sigma = 1$ in the model. Solid line: results of the fit on the points obtained with the model density. The experimental volume is shown by the dashed line.

4. Localization radius and bulk properties

So far, we have found that the SCD is receptive to a change in the valence density. We now explore to what extent the valence density is influenced by a change in the SCD, and show that the LR has a big effect on the cohesive properties of the solid state. We fix our set of large core pseudopotentials obtained with the $3d^44s^04p^0$ configuration, and vary the SCD in equation (1). We take first the SCD of the $3d^24s^24p^0$ or $3d^04s^24p^2$ configurations. The equilibrium volume is found to increase when the SCD localization radius decreases (figure 3, empty circles). Second, we show that by artificially enforcing the localization of the SCD, one is able to tune the volume expansion associated with the large core pseudopotentials. To this end we define the model density $\rho_{\rm M}$ which we make depend on one single parameter σ:

$$\rho_{\rm M}(r) = \sigma^3 \rho_{\rm ref}(pr). \qquad (3)$$

Table 3. Face centered cubic copper: same as table 2. FSCA + NLCC results are obtained with the optimal $3d^{10}4s^1$ configuration, or with $3d^8\ 4s^0$.

			FSCA + NLCC		
	GGA	LDA	$3d^{10}4s^1$	$3d^84s^0$	Exp
$\langle r \rangle$	0.396	0.397	0.398	0.392	
V_{eq}	11.93	10.88	10.84	11.04	11.68 [29]
B	142	190	184	173	142 [29]

σ controls the localization radius, and the reference SCD ρ_{ref} is chosen to be the pseudodensity[5] of the atom with configuration $3d^44s^04p^0$. We have inserted $\rho_{SC} = \rho_M$ into equation (1), all other parameters of the pseudopotentials being kept constant (figure 3, empty circles for $\sigma = 1.2$ and 1.4). Our conclusion is valid over a wide range of localization radii: the more localized our SCD, the larger the equilibrium volume.

5. Construction criteria for large core pseudopotentials

In the previous section we varied only the SCD. We now change both the pseudopotentials and the SCD in a consistent manner and investigate the cohesive properties. We compare two sets of large core pseudopotentials for titanium and copper (tables 2 and 3). The FSCA + NLCC results are much closer to the small core LDA reference calculation when the 3d occupation numbers are similar in the solid and in the atomic configuration used to generate the large core pseudopotentials. Only in this case (optimal atomic configuration) are the LR and the 3d occupation number consistent with each other in the solid. The use of large core pseudopotentials for a given atom can be *a posteriori* justified by inspection of the occupation number of 3d orbitals of this atom.

With the optimal atomic configuration, the relative error on the volume is drastically reduced by one order of magnitude in titanium, and is three times smaller in copper (tables 2 and 3). By construction, the FSCA + NLCC scheme cannot yield *exactly* the same value as the reference calculation. The residual error bar comes from the large cutoff radius of the 4s (4p) pseudopotentials which cannot be chosen in the inert region (see footnote 2). The 4s component of the KS orbitals is approximate in the semicore region (figure 1), as well as its hybridization with the d orbitals. The valence density is consequently not exact (with respect to the reference calculation) in the semicore region for any large core pseudopotential, and the corresponding error amounts to ≈2% on the volume.

The bulk moduli are also much improved (tables 2 and 3). This quantity is particularly sensitive in copper, and evolves from 190 GPa in LDA to 142 GPa in GGA. With the optimal atomic configuration, the discrepancy between large and small core pseudopotentials amounts to only 3%.

[5] We have fitted the 3s and 3p pseudo-orbitals with the expression $r^l P(r)\, e^{-br}$, where P is a polynomial of order 6, b a positive real number and l the angular momentum, and built the semicore density $\rho_{ref}(r) = 2(P_{3s}(r)\, e^{-b_{3s}r})^2 + 6(P_{3p}(r)\, e^{-b_{3p}r})^2$.

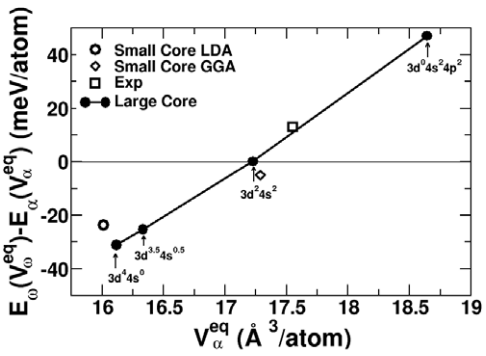

Figure 4. Titanium: energy difference (meV/atom) between the low (α) and high (ω) pressure phases in function of the equilibrium volume of the α phase (Å^3/atom). Solid line: calculated with the large core pseudopotentials. Empty circle and diamond: LDA and GGA results for the small core pseudopotentials. Empty square: experiment [22][6] .

Lastly, we study phase stability. In the low temperature experiments on titanium [30, 31] the low pressure hcp phase is found to be more stable than the high pressure ω phase, and the energy difference $E_\omega - E_\alpha$ is positive (table 2). Contrastingly, the reference calculation including semicore states in the valence erroneously predicts that the ω phase is the most stable one, as shown by the negative sign of the energy difference both in the LDA and the GGA (table 2), in agreement with most previous theoretical works [32–39]. The main reason why usual xc functionals fail to reproduce the tiny energy difference between ω and α phases is that they fail to reproduce the experimental volume [22].

The energy difference $E_\omega - E_\alpha$ is a particularly stringent test for the FSCA + NLCC scheme. As reported in figure 4, most calculations (filled circles) are in qualitative disagreement with the reference results (small core LDA, empty circles). This illustrates the need, when studying transition metals with large core pseudopotentials, to closely compare the results with those obtained with a set of reference small core pseudopotentials and the same xc functional. In fact large core pseudopotential results can be fortuitously in better agreement with experiment than more precise small core pseudopotential results. However, differences between theoretical results and experiment come from the xc approximation and should not be corrected by pseudopotentials but with xc functionals more suitable for solids. Only pseudopotentials designed with the optimal atomic configuration are able to recover both the sign and the absolute value of the relative energy of the LDA reference calculation (table 2).

Our theoretical results reveal the linear dependence of $E_\omega - E_\alpha$ on the volume (figure 4, solid line), and give a unified picture of the various calculations. Furthermore, the experimental value (empty square) is gratifyingly consistent with the alignment. The link between SCD localization radius, equilibrium volume and energy difference provides an explanation for the scattering of the theoretical data reported in the literature [33–36, 40–43]: $E_\omega - E_\alpha$ ranges from −13 to 3 meV in the GGA, ±160% with respect to our

[6] The value is deduced from the data of [29] and [28], see [46].

reference value. Figure 4 illustrates the need for an exchange and correlation functional yielding more accurate equilibrium volumes [49–51]. The usual functionals, even the GGA, are not capable of reproducing the stability of titanium phases.

6. Conclusion

In conclusion, we have defined a localization radius for the semicore density, and found it to be an important parameter of the equilibrium properties of transition and noble metals. Moreover we have shown that the localization radius of the SCD is controlled by the occupation number of the 3d electronic subshell both in the atom and in the solid. We believe this finding to also hold for the 4d elements

We propose a construction criterion for large core pseudopotentials based on the SCD localization radius. The construction steps are as follows: (i) In the solid, the number of electrons in the 3d electronic states is obtained from a calculation with the 3sp electrons included in the valence. (ii) The atomic configuration with that 3d occupation number is chosen as the reference one to develop the large core pseudopotentials. We have shown that this procedure minimizes the loss of accuracy as it ensures that the SCD is close to the reference one. In the course of a simulation, a check of the occupation number of the 3d orbital can also be used to *a posteriori* justify the use of a large core pseudopotential.

This will be useful for studying surfaces or defects, where atoms far from the surface/impurity are bulk atoms, for which a large core pseudopotential is sufficient. This leads to a significant reduction of the computational burden, while controlling the accuracy of the calculations.

Acknowledgments

This work has been supported by the EU's 6th Framework Programme through the NANOQUANTA Network of Excellence. We thank Jean-Claude Toledano, Marie-Bernadette Lepetit, Stefano Baroni and Olivier Hardouin-Duparc for fruitful discussions. Our pseudopotentials have been developed with the (modified) Dfhipp package [44, 45], and ground-state results obtained with the (modified) espresso package [46, 47]. Computer time has been granted by CEA/DSM on the NEC SX8 (project p93).

References

[1] Hohenberg P and Kohn W 1964 *Phys. Rev.* B **136** 864
[2] Kohn W and Sham L 1965 *Phys. Rev.* A **140** 1133
[3] Kübler J and Eyert V 1992 Electronic structure calculations *Electronic and Magnetic Properties of Metals and Ceramics* ed K H J Buschow (Weinheim: VCH) pp 1991–6
[4] Pickett W 1989 *Comput. Phys. Rep.* **9** 115
[5] Louie S G, Froyen S and Cohen M L 1982 *Phys. Rev.* B **26** 1738
[6] Zhu J, Wang X W and Louie S G 1992 *Phys. Rev.* B **45** 8887
[7] Cho J-H and Scheffler M 1996 *Phys. Rev.* B **53** 10685
[8] Han S, Zepeda-Ruiz L A, Ackland G J, Car R and Srolovitz D J 2002 *Phys. Rev.* B **66** 220101(R)
[9] Moroni E G, Kresse G, Hafner J and Furthmüller J 1997 *Phys. Rev.* B **56** 15629
[10] Ballone P and Jones R 1995 *Chem. Phys. Lett.* **233** 632
[11] Oda T, Pasquarello A and Car R 1998 *Phys. Rev. Lett.* **80** 3622
[12] Porezag D, Pederson M R and Liu A Y 1999 *Phys. Rev.* B **60** 14132
[13] Engel E, Höck A and Varga S 2001 *Phys. Rev.* B **63** 125121
[14] Fu C-C, Willaime F and Ordejón P 2004 *Phys. Rev. Lett.* **92** 175503
[15] Bachelet G B, Hamann D R and Schlüter M 1982 *Phys. Rev.* B **26** 4199
[16] Goedecker S and Maschke K 1992 *Phys. Rev.* A **45** 88
[17] Troullier N and Martins J L 1991 *Phys. Rev.* B **43** 1993
[18] Blöchl P E, Jepsen O and Andersen O K 1994 *Phys. Rev.* B **49** 16223
[19] Ceperley D M and Adler B J 1980 *Phys. Rev. Lett.* **45** 566
[20] Perdew J P and Zunger A 1981 *Phys. Rev.* B **23** 5048
[21] Perdew J P, Burke K and Ernzerhof M 1996 *Phys. Rev. Lett.* **77** 3865
[22] Trinité V, Vast N, Hayoun M, Dammak H and Toledano J 2008 in preparation
[23] Spreadborough J and Christian J 1959 *Proc. Phys. Soc. LXXIV* **5** 609
[24] Jamieson J 1963 *Sciences* **140** 72
[25] Fisher E S and Renken C J 1964 *Phys. Rev.* **135** A482
[26] Chase M W, Davies C A, Downey J R, Frurip D J, McDonald R A and Syverud A N 1985 JANAF Thermochemical Tables *J. Phys. Chem. Ref. Data* **14** Suppl. I
[27] Sanchez-Portal D, Artacho E and Soler J 1995 *Solid State Commun.* **95** 685
[28] Berggren K-F, Manninen S and Paakkari T 1973 *Phys. Rev.* B **8** 2516
[29] Kittel C 1972 *Introduction à la physique du solide* 3rd edn (Paris: Dunod univer)
[30] Errandonea D, Meng Y, Somayazulu M and Häusermann D 2005 *Physica* B **355** 116
[31] Dewaele A 2006 private communication
[32] Ahuja R, Wills J M, Johansson B and Eriksson O 1993 *Phys. Rev.* B **48** 16269
[33] Jomard G, Magaud L and Pasturel A 1998 *Phil. Mag.* **77** 67
[34] Greeff C W, Trinkle D and Albers R 2001 *J. Appl. Phys.* **90** 2221
[35] Kutepov A L and Kutepova S G 2003 *Phys. Rev.* B **67** 132102
[36] Trinkle D R, Hennig R G, Srinivasan S G, Hatch D M, Jones M D, Stokes H T, Albers R C and Wilkins J W 2003 *Phys. Rev. Lett.* **91** 025701
[37] Rudin S P, Jones M D and Albers R C 2004 *Phys. Rev.* B **69** 094117
[38] Hennig R G, Tinkle D, Bouchet J, Srinivasan S, Albers R and Wilkins J 2005 *Nat. Mater.* **4** 129
[39] Trinkle D R, Hatch D M, Stokes H T, Hennig R G and Albers R C 2005 *Phys. Rev.* B **72** 014105
[40] Aguayo A, Murrieta G and deCoss R 2002 *Phys. Rev.* B **65** 092106
[41] Nishitani S, Kawabe H and Aoki M 2001 *Mater. Sci. Eng.* A **312** 77
[42] Jona F and Marcus P 2005 *Phys. Status Solidi* **15** 3077
[43] Trinkle D R, Jones M D, Hennig R G, Rudin S P, Albers R C and Wilkins J W 2006 *Phys. Rev.* B **73** 094123
[44] Fuchs M *et al* http://www.fhi-berlin.mpg.de/th/fhi98md/fhi98PP/
[45] Fuchs M and Scheffler M 1999 *Comput. Phys. Commun.* **119** 64
[46] Baroni S *et al* http://www.pwscf.org
[47] Baroni S, deGironcoli S, Corso A D and Giannozzi P 2001 *Rev. Mod. Phys.* **73** 515
[48] Trinité V 2006 *PhD Thesis* Ecole Polytechnique, Palaiseau, France http://www.imprimerie.polytechnique.fr/Theses/Files/Trinite.pdf
[49] Perdew J P, Ruzsinsky A, Csonka G I, Vydrov O A, Scuseria G E, Constantin L A, Zhou X and Burke K 2008 *Phys. Rev. Lett.* **100** 136406
[50] Wu Z and Cohen R E 2006 *Phys. Rev.* B **73** 235116
[51] Paier J, Marsman M and Kresse G 2007 *J. Chem. Phys.* **127** 024103